Electrochemical and Spectroscopic Studies of (P)Rh(R)(L) and $[(P)Rh(L)_2]^+$ Where P Is the Dianion of Octaethyl- or Tetraphenylporphyrin, R Is a σ-Bonded Alkyl Group, and L Is Triphenylphosphine or Dimethylphenylphosphine

K. M. Kadish,* C. Araullo, and C.-L. Yao

Department of Chemistry, University of Houston, Houston, Texas 77004

Received December 17, 1987

The electrochemistry and spectroelectrochemistry of (P)Rh(R), (P)Rh(R)(L), and $[(P)Rh(L)_2]^+$ where P is the dianion of octaethylporphyrin (OEP) or tetraphenylporphyrin (TPP), R is CH_3, C_2H_5, or C_4H_9, and L is triphenylphosphine or dimethylphenylphosphine are reported. At polarographic concentrations of (P)Rh(R) ($\sim 10^{-3}$ M), the binding of one triphenylphosphine ligand and the formation of (P)Rh(R)(PPh_3) are observed. This contrasts to lower porphyrin concentrations where the bis(triphenylphosphine) adduct $[(P)Rh(PPh_3)_2]^+$ is formed in solution. Formation constants for the conversion of (P)Rh(R) to (P)Rh(R)(PPh_3) were calculated by using electrochemical and spectroscopic methodologies and varied between 1.0 and 4.0×10^3 depending upon the porphyrin macrocycle (OEP or TPP), the specific R group, and the solvent (methylene chloride or benzonitrile). The electroreduction of (P)Rh(R)(PPh_3) initially leads to a porphyrin π radical and the transient formation of $[(P)Rh(R)(PPh_3)]^-$ was spectrally characterized on the thin-layer electrochemical time scale. The formation of a porphyrin π radical is also observed after reduction of $[(TPP)Rh(PPhMe_2)_2]^+$. This reaction was characterized by thin-layer spectroelectrochemistry and provides the first example for reduction of a non-σ-bonded Rh(III) porphyrin at the porphyrin π-ring system.

Introduction

Rhodium porphyrin complexes with σ-bonded alkyl or aryl groups can undergo up to two reversible reductions at the porphyrin π-ring system.[1-3] This electrochemical behavior contrasts with that for rhodium porphyrins containing bound dioxygen[4] or nitrogen[5] donor ligands such as dimethylamine or pyridine. For these complexes there is an irreversible reduction at the Rh(III) center and the final electroreduction product is a Rh(II) porphyrin dimer.

The potentials for electroreduction of rhodium porphyrins also depend upon the nature of the fifth and sixth axial ligands.[1-5] For example, Rh(III) porphyrin complexes with anionic or nitrogen donor ligands are irreversibly reduced at potentials that vary between -0.70 and -1.24 V vs SCE depending upon the specific porphyrin ring and the counterion associated with Rh(III). In contrast, $E_{1/2}$ values for reduction of alkyl σ-bonded Rh(III) complexes are located at substantially more negative potentials which range between -1.40 and -1.45 V vs SCE.

The negative shift in half-wave potentials for reduction of the σ-bonded rhodium porphyrins is consistent with voltammetric data for the reduction of other transition-metal porphyrin complexes.[1,6] For example, the reduction of (TPP)$FeClO_4$ occurs at $E_{1/2} = 0.24$ V in CH_2Cl_2[7] while (TPP)Fe(C_6H_5)[8] is reversibly reduced at $E_{1/2} = -0.76$ V in the same solvent, supporting electrolyte system. Likewise, the irreversible reduction of (TPP)CoCl occurs at $E_{pc} = 0.57$ V in CH_2Cl_2[9] while $E_{1/2}$ for (TPP)Co(C_6H_5) reduction is shifted to -1.30 V under the same experimental conditions.[10]

This paper concentrates on the electrochemistry and spectroelectrochemistry of (P)Rh(R)(L) and $[(P)Rh(L)_2]^+$ where P is the dianion of octaethylporphyrin (OEP) or tetraphenylporphyrin (TPP), R is CH_3, C_2H_5, or C_4H_9, and L is triphenylphosphine or dimethylphenylphosphine. The reactions of (OEP)RhCl[11] with triphenylphosphine and tributylphosphine as well as (TPP)Rh(O_2)[4] with triphenylphosphine have been reported. The first ligand addition reaction of these two porphyrins with triphenylphosphine results in the formation (TPP)Rh(O_2)(PPh_3) or (OEP)Rh(Cl)(PPh_3), the latter of which was crystallographically characterized.[6] The second ligand addition results in the formation of $[(TPP)Rh(PPh_3)_2]^+$ and $[(OEP)Rh(PPh_3)_2]^+$.

A two-step addition of triphenylphosphine to (TPP)Rh(R) and (OEP)Rh(R) may also occur depending upon the experimental conditions. The first ligand addition reaction results in formation of (TPP)Rh(R)(PPh_3) or (OEP)Rh(R)(PPh_3) as shown by eq 1.

$$(P)Rh(R) + PPh_3 \rightleftharpoons (P)Rh(R)(PPh_3) \quad (1)$$

The binding of a second ligand only occurs at low porphyrin concentrations and gives $[(P)Rh(PPh_3)_2]^+$ as a final product. This reaction is shown in eq 2.

$$(P)Rh(R)(PPh_3) + PPh_3 \rightarrow [(P)Rh(PPh_3)_2]^+ + R^- \quad (2)$$

In this paper, formation constants were calculated for triphenylphosphine binding according to eq 1 and the electrochemistry and spectroelectrochemistry of each six-coordinate (P)Rh(R)(PPh_3) complex were investigated in methylene chloride (CH_2Cl_2) and benzonitrile (PhCN) containing up to 1000 equiv of triphenylphosphine. The bis(dimethylphenylphosphine) adduct $[(P)Rh(PPhMe_2)_2]^+$

(1) Anderson, J. E.; Yao, C.-L.; Kadish, K. M. *J. Am. Chem. Soc.* **1987**, *109*, 1106.
(2) Anderson, J. E.; Liu, Y.-H.; Kadish, K. M. *Inorg. Chem.* **1987**, *26*, 4174.
(3) Kadish, K. M.; Anderson, J. E.; Yao, C.-L. *Inorg. Chem.* **1986**, *25*, 1277.
(4) Anderson, J. E.; Yao, C.-L.; Kadish, K. M. *Inorg. Chem.* **1986**, *26*, 3224.
(5) Kadish, K. M.; Yao, C.-L.; Anderson, J. E.; Cocolios, P. *Inorg. Chem.* **1985**, *24*, 4515.
(6) Guilard, R.; Lecomte, C.; Kadish, K. M. *Struct. Bonding (Berlin)* **1987**, *64*, 205-268.
(7) Kadish, K. M. *J. Electroanal. Chem.* **1984**, *168*, 261.
(8) Lançon, D.; Cocolios, P.; Guilard, R.; Kadish, K. M. *J. Am. Chem. Soc.* **1984**, *106*, 4472.
(9) Kadish, K. M.; Lin, X. Q.; Han, B. C. *Inorg. Chem.* **1987**, *26*, 4161.
(10) Callot, H. J.; Cromer, R.; Louati, A.; Gross, M. *Nouv. J. Chim.* **1985**, *8*, 765.
(11) Thackray, D. C.; Ariel, S.; Leung, T. W.; Menon, K.; James, B. R.; Trotter, J. *Can. J. Chem.* **1986**, *64*, 2440.

0276-7333/88/2307-1583$01.50/0

Table I. UV-Visible Spectra of (P)Rh(R), (P)Rh(R)(PPh_3), and $[(P)Rh(PPh_3)_2]^+$ in CH_2Cl_2 and PhCN

compound	λ_{max}, nm ($10^{-3}\epsilon$)							
	CH_2Cl_2				PhCN			
(TPP)Rh(CH_3)		411 (192)	520 (20.4)	549 (1.6)		420 (193)	534 (18.6)	569 (4.6)
(TPP)Rh(CH_3)(PPh_3)	369 (48.6)	439 (107)	549 (11.7)	590 (7.1)	370 (59.1)	439 (131)	548 (13.1)	595 (8.4)
(TPP)Rh(C_2H_5)		410 (201)	519 (21.5)	545 (5.3)		417 (192)	522 (18.6)	557 (3.0)
(TPP)Rh(C_2H_5)(PPh_3)	376 (49.3)	439 (109)	548 (11.5)	586 (8.4)	377 (57.0)	436 (109)	545 (12.4)	596 (6.2)
(TPP)Rh(C_4H_9)		411 (199)	518 (21.6)	544 (3.1)		416 (196)	522 (19.6)	
(TPP)Rh(C_4H_9)(PPh_3)	376 (59.0)	438 (110)	548 (10.8)	594 (7.2)	378 (58)	438 (94.3)	546 (11.3)	595 (6.2)
(OEP)Rh(CH_3)		393 (106)	511 (10.7)	542 (30.0)		401 (140)	516 (13.6)	548 (25.6)
(OEP)Rh(CH_3)(PPh_3)	363 (57.4)	428 (75.2)	535 (15.4)	558 (9.4)	364 (69.2)	426 (69.2)	534 (14.2)	558 (10.3)
(OEP)Rh(Cl)(PPh_3)[a]			529 (19.1)[a]	560 (23.4)[a]				
$[(OEP)Rh(PPh_3)_2]^+$		431	537 (18.6)[a]	568 (12.9)[a]				
(TPP)Rh(O_2)[b]		418 (188)	534 (18.1)	574 (3.2)		428 (221)	538 (19.8)	573 (4.6)
(TPP)Rh(O_2)(PPh_3)[b]		437 (191)	546 (13.9)	584 (8.0)		438 (149)	556 (11.2)	597 (10.6)
$[(TPP)Rh(PPh_3)_2]^+$	362 (18.0)	445 (154)	558 (9.8)	597 (9.4)				
$[(TPP)Rh(PPhMe_2)_2]^+$	359 (31.6)	444 (138)	555 (8.0)	594 (9.7)				

[a] Reference 11. [b] Reference 4.

was also synthesized and electrochemically investigated.

Experimental Section

Materials. All solvents and supporting electrolytes used for electrochemical measurements were purified as described in the literature.[1] The supporting electrolyte was 0.2 M tetrabutylammonium perchlorate (TBAP) for cyclic voltammetric measurements, bulk solution electrolysis, and spectroelectrochemical measurements. Triphenylphosphine (PPh_3) (Aldrich) was twice recrystallized from ethanol and dried in a vacuum oven at 40 °C prior to use. Dimethylphenylphosphine ($PPhMe_2$) was purchased from Aldrich Chemical Co. and used as obtained.

The σ-bonded (P)Rh(R) complexes were prepared by literature methods using appropriate iodo-alkylhydrocarbons.[1,2] Six-coordinate $[(TPP)Rh(PPh_3)_2]^+$ was obtained by adding excess PPh_3 to (TPP)Rh(O_2) in CH_2Cl_2, 0.2 M TBAP, and stirring for 2 h at room temperature. The reaction was monitored by UV-visible spectroscopy and thin-layer chromatography. The product was purified on an activated alumina column and is characterized by UV-visible bands at 362, 445, 558, and 597 nm. In addition to porphyrin resonances, the ^1H NMR spectrum has the following triphenylphosphine peaks in $CDCl_3$: δ 6.47 (*m*-phenyl, t, 12 H), 6.93 (*p*-phenyl, t, 6 H), and 7.72 (*o*-phenyl, d, 12 H).

The dimethylphenylphosphine adduct $[(TPP)Rh(PPhMe_2)_2]^+$ was prepared by the same method used for preparation of $[(TPP)Rh(PPh_3)_2]^+$ and shows UV-visible bands at 359, 444, 555, and 594 nm. The ^1H NMR spectrum of this complex has the following dimethylphenylphosphine peaks in $CDCl_3$: δ, 1.85 (*p*-CH_3, t, 12 H), 6.97 (*p*-phenyl, t, 2 H), 6.45 (*o*-phenyl, t, 4 H), and 3.83 (*p*-phenyl, m, 4 H) in addition to the normal porphyrin peaks.

Instrumentation and Methods. The utilized electrochemical instrumentation[1] and electrochemical cell designs[1,12] are described in the literature. Potentials are reported at 23 ± 1 °C and were measured vs a saturated calomel electrode (SCE). UV-visible spectra were recorded with a Tracor Northern 1710 spectrometer/multichannel analyzer or with an IBM 9430 spectrophotometer using cells adapted for inert-atmosphere measurements. The thin-layer cell used for spectroscopic measurements had a calibrated path length of 0.17 mm, while the cell used for spectroelectrochemistry had a path length of 0.27 mm. NMR spectra were taken on a Nicolet FT 300 spectrometer.

Results and Discussion

Spectral Monitoring of the Reaction between (P)Rh(R) and Triphenylphosphine. Figure 1 shows the UV-visible spectral changes that occur during a titration of 2.6×10^{-3} M (TPP)Rh(C_2H_5) with PPh_3 in CH_2Cl_2. The initial (TPP)Rh(C_2H_5) complex has absorption bands at 410, 519, and 545 nm. When PPh_3 is added to this solution, new absorption peaks appear at 376, 439, 548, and 586 nm. The spectra continue to change as indicated by arrows in Figure 1 until 200 equiv of PPh_3 have been added to the solution. At this point, the spectra become invariant, indicating the complete formation of (TPP)Rh(C_2H_5)(PPh_3) in solution.

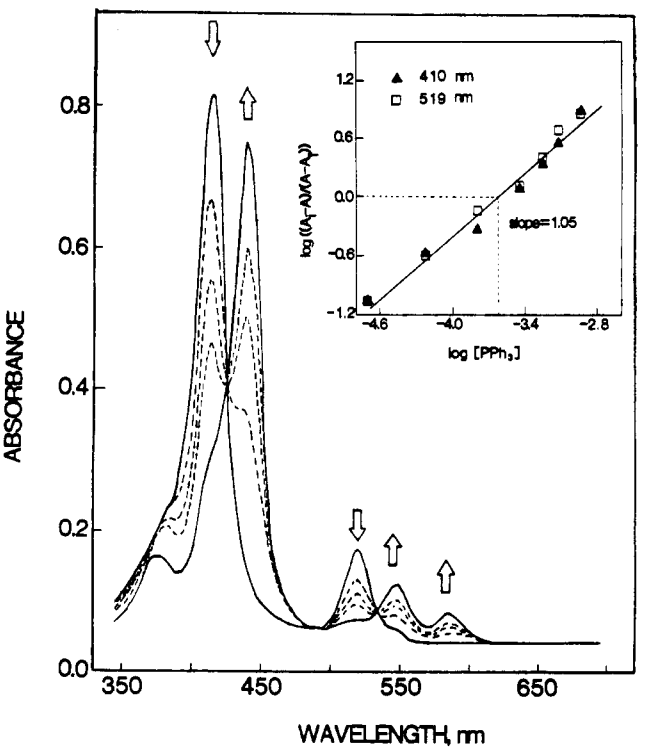

Figure 1. (a) Electronic absorption spectra taken during the titration of 2.6×10^{-3} M (TPP)Rh(C_2H_5) with PPh_3 in CH_2Cl_2. (b) Analysis of spectral data for the titration of (TPP)Rh(C_2H_5) with PPh_3. Wavelengths analyzed: 410 nm (▲); 519 nm (□).

A linear least-squares treatment of the spectral data at 410 and 519 nm is shown in the insert of Figure 1. The same relationship is obtained at both wavelengths, and the slope of the line gives a value of 1.05 and a formation constant of $K = 4.0 \times 10^3$ for reaction 1. Similar types of spectral changes were observed during titrations of (TPP)Rh(CH_3), (TPP)Rh(C_4H_9), and (OEP)Rh(CH_3) with PPh_3 in CH_2Cl_2, and spectral data of the initial (P)Rh(R) and the generated (P)Rh(R)(L) complexes are listed in Table I. The formation constants for addition of triphenylphosphine to each (P)Rh(R) complex were also similar and varied between 1.0 and 4.0×10^3 in CH_2Cl_2.

As seen in Table I, the Soret bands of (TPP)Rh(R) are red-shifted by 28 ± 1 nm upon formation of (TPP)Rh(R)(PPh_3). There is also a shoulder on the Soret band that

(12) Lin, X. Q.; Kadish, K. M. *Anal. Chem.* **1985**, *57*, 1498.

Table II. ^{1}H NMR Data (δ) of (P)Rh(R) and (P)Rh(R)(PPh$_3$) in C_6D_6[a]

compd	complex: (P)Rh(R)[b]	complex: (P)Rh(R)(PPh$_3$)
(TPP)Rh(CH$_3$)	−5.54 (3 H, d)	−5.94 (3 H, m)[c]
(TPP)Rh(C$_2$H$_5$)	−4.61 (2 H, m)	−5.06 (2 H, m)[c]
	−4.19 (3 H, t)	−4.06 (3 H, t)
(TPP)Rh(C$_4$H$_9$)	−4.60 (2 H, m)	−4.84 (2 H, m)[c]
	−4.18 (2 H, p)	−4.20 (2 H, p)
	−1.57 (2 H, h)	−1.51 (2 H, h)
	−0.81 (3 H, t)	−0.79 (3 H, t)
(OEP)Rh(CH$_3$)	−6.04 (3 H, d)	−6.55 (3 H, d)

[a] Only resonance of R ligand are listed. [b] References 1 and 2. [c] Multiplet, peaks not resolved.

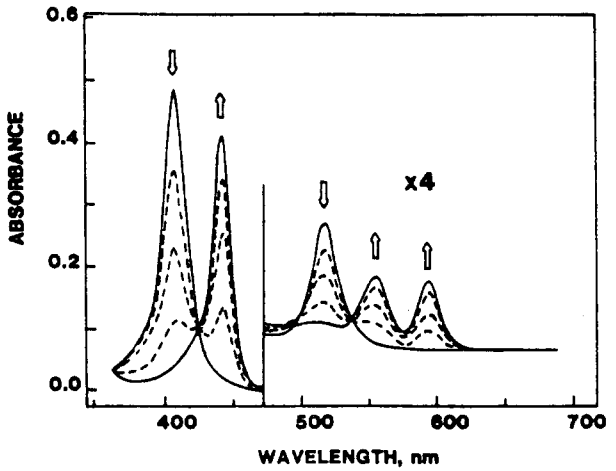

Figure 2. Electronic absorption spectra taken during the titration of 1.3 × 10^{-5} M (TPP)Rh(CH$_3$) with PPh$_3$ in CH$_2$Cl$_2$.

appears between 369 and 376 nm. Similar types of spectral changes occur upon addition of PPh$_3$ to solutions of (P)Rh(R) in PhCN, but, in this solvent, the initial σ-bonded complex exists as the six-coordinate solvated adduct (P)Rh(R)(PhCN). Thus, the overall ligand binding reaction under these conditions is given by eq 3. The Soret

$$\text{(P)Rh(R)(PhCN)} + \text{PPh}_3 \rightleftharpoons \text{(P)Rh(R)(PPh}_3\text{)} + \text{PhCN} \quad (3)$$

band of (OEP)Rh(CH$_3$)(PhCN) is located at 401 nm in PhCN while that of (TPP)Rh(R)(PhCN) in PhCN varies between 416 and 420 nm depending upon the specific R group. These latter values are red-shifted by 5–9 nm with respect to the same (TPP)Rh(R) complexes in CH$_2$Cl$_2$. Differences of 4–22 nm are also observed between the visible bands of (P)Rh(R) in CH$_2$Cl$_2$ and (P)Rh(R)(PhCN) in PhCN. On the other hand, virtually identical spectra are obtained for (P)Rh(R)(PPh$_3$) in each of the two investigated solvents.

The formation of (P)Rh(R)(PPh$_3$) as the first product in the ligand binding reaction with triphenylphosphine is also demonstrated by ^{1}H NMR spectra of the products. The methyl group of (TPP)Rh(CH$_3$) in C_6D_6 is a doublet at −5.54 ppm[2] but shifts to −5.94 ppm in the presence of 1.5 equiv of PPh$_3$. A similar high-field shift is observed for each of the four investigated (P)Rh(R)(PPh$_3$) complexes. The shift of the α proton is about 0.2–0.5 ppm upon going from (TPP)Rh(R) to (TPP)Rh(R)(PPh$_3$). These resonances are listed in Table II.

When the concentration of (TPP)Rh(R) is less than 2 × 10^{-5} M, only [(TPP)Rh(PPh$_3$)$_2$]$^+$ is observed as a product of the triphenylphosphine titration. This ligand binding reaction occurs via an overall irreversible one-step process as shown in Figure 2 for the case of 1.3 × 10^{-5} M (TPP)Rh(CH$_3$) in CH$_2$Cl$_2$. No detectable spectral intermediates are observed during this titration, and the final spectrum is identical with that of [(TPP)Rh(PPh$_3$)$_2$]$^+$ (which can be chemically synthesized from (TPP)Rh(O$_2$) as described in the Experimental Section of the paper). The same types of spectral changes occur during the titration of 10^{-5} M (TPP)Rh(CH$_3$) or (TPP)Rh(C$_2$H$_5$) with PPh$_3$, and the final spectra in both cases correspond to that of [(TPP)Rh(PPh$_3$)$_2$]$^+$ which has bands at 362, 445, 558, and 597 nm (see Table I). The fate of the σ-bonded R group after dissociation is unknown. However, whatever the fate of this liberated ligand, it is both spectrally and electrochemically nondetectable.

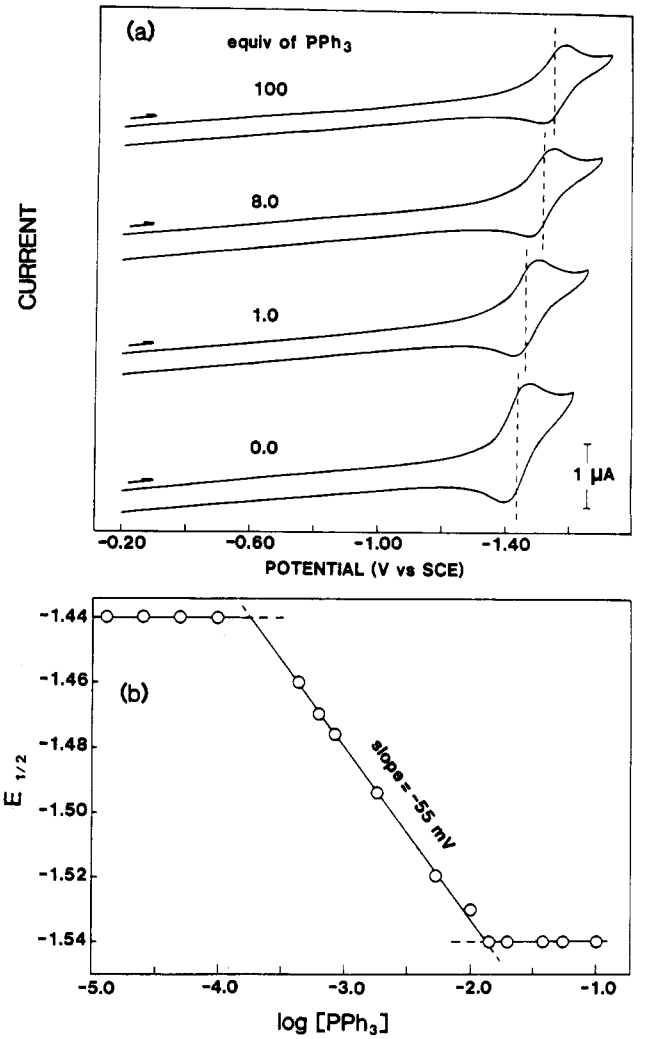

Figure 3. (a) Cyclic voltammograms of 5.7 × 10^{-4} M (TPP)Rh(CH$_3$) in CH$_2$Cl$_2$ containing various equivalents of PPh$_3$ and 0.2 M TBAP. Scan rate = 0.1 V/s. (b) Analysis of electrochemical data for the titration of (TPP)Rh(CH$_3$) with PPh$_3$.

Electrochemistry of (P)Rh(R) in CH$_2$Cl$_2$ or PhCN Containing Triphenylphosphine. (TPP)Rh(R) where R = CH$_3$, C$_2$H$_5$, or C$_4$H$_9$ undergoes two reversible one-electron reductions in THF and PhCN.[1,2] The first occurs at $E_{1/2}$ = −1.42 ± 0.02 V and the second at $E_{1/2}$ = −1.90 ± 0.02 V. Controlled potential electrolysis coupled with UV–visible and ESR spectral monitoring of the reduction products indicates that both reductions are porphyrin ring centered and generate first a π radical followed by a dianion.[2] Two reductions also occur in CH$_2$Cl$_2$, but only the first reaction is well-defined due to the negative potential cutoff of the solvent.

Half-wave potentials for the first reduction of the (P)Rh(R)(PPh$_3$) complexes are more negative than $E_{1/2}$ for

Table III. Formation Constants for Binding of PPh_3 by (P)Rh(R) in CH_2Cl_2 and PhCN at 23 ± 1 °C[a]

porphyrin, P	R	solv CH_2Cl_2	solv PhCN
TPP	CH_3	3.9×10^3	1.0×10^2
	C_2H_5	1.2×10^3	4.2×10^2
	C_4H_9	1.0×10^3	4.3×10^2
OEP	CH_3	1.8×10^3	2.4×10^2

[a] According to reaction 1 in text. Calculated from analysis of electrochemical titration data.

reduction of the corresponding five-coordinate (P)Rh(R) species in the absence of triphenylphosphine. Also, a plot of $E_{1/2}$ vs log [PPh_3] gives a slope of −50 to −57 mV for reduction of (P)Rh(R)(PPh_3) in CH_2Cl_2 or PhCN containing 2–100 equiv of PPh_3. This is shown in Figure 3 for the case of (TPP)Rh(CH_3). The −55 mV slope obtained in the $E_{1/2}$ vs log [PPh_3] plot is comparable with a theoretical slope of −59 mV per decade change in ligand concentration when a one-electron reduction is coupled with a single-ligand dissociation.[13] The data in Figure 3 indicate that (TPP)Rh(CH_3)(PPh_3) is the rhodium species reduced at the electrode surface and that the triphenylphosphine ligand dissociates after the addition of one electron to the neutral six-coordinate complex. This electrode reaction is given by eq 4.

$$(TPP)Rh(CH_3)(PPh_3) + e \rightleftharpoons [(TPP)Rh(CH_3)]^- + PPh_3 \quad (4)$$

The $E_{1/2}$ for reduction of (TPP)Rh(CH_3)(PPh_3) is invariant at −1.54 V in CH_2Cl_2 containing between 100 and 1000 equiv of triphenylphosphine. Under these conditions the overall electrochemical reaction can be described as shown in eq 5. Electrochemically monitored titrations of

$$(TPP)Rh(R)(PPh_3) + e \rightleftharpoons [(TPP)Rh(R)(PPh_3)]^- \quad (5)$$

10^{-3} M (TPP)Rh(C_2H_5), (TPP)Rh(C_4H_9), and (OEP)Rh(CH_3) with PPh_3 were also carried out in CH_2Cl_2 and PhCN and gave similar results as shown in Figure 3 for the case of (TPP)Rh(CH_3).

Formation constants for the binding of triphenylphosphine to (TPP)Rh(R) and (OEP)Rh(R) in both CH_2Cl_2 and PhCN were calculated by using electrochemical data of the type shown in Figure 3 and are listed in Table III. As seen in this table, the binding constants are smaller by about 1 order of magnitude in PhCN than in CH_2Cl_2. This is consistent with coordination of PhCN by (P)Rh(R) and the fact that the actual ligand binding reaction in PhCN is a displacement reaction as shown by eq 3. A similar solvent effect on formation constants has been reported for the binding of PPh_3 by (TPP)Rh(O_2).[4] However, in the case of these reactions, the equilibrium constant for formation of (TPP)Rh(O_2)(PPh_3) from (TPP)Rh(O_2) is 3.3×10^5, some 2 orders of magnitude larger than values observed for the addition of PPh_3 to (TPP)Rh(R). This difference is expected since the σ-bonded alkyl ligand is a better electron donor than O_2^- and will tend to increase to a greater extent the electron density on the metal, thus reducing the acceptor properties of the rhodium center.

Thin-layer spectroelectrochemistry was utilized to characterize electrode reactions of the type shown in eq 5, and examples of the obtained spectral changes are illustrated in Figure 4 for the (TPP)Rh(CH_3)(PPh_3) reduction. The neutral complex has UV–visible absorption bands at 376, 439, 549, and 590 nm (see Table I). These bands decrease in intensity upon reduction at −1.65 V, and new bands for [(TPP)Rh(CH_3)(PPh_3)]$^-$ appear at 379, 437, 549, 594, and 608 nm. The 437, 549, and 594 bands are similar to those of [(TPP)Rh(CH_3)]$^-$, but the bands at 379 and 608 nm are only found for the six-coordinate species. Similar types of spectral changes were obtained for all three of the investigated (TPP)Rh(R)(PPh_3) complexes.

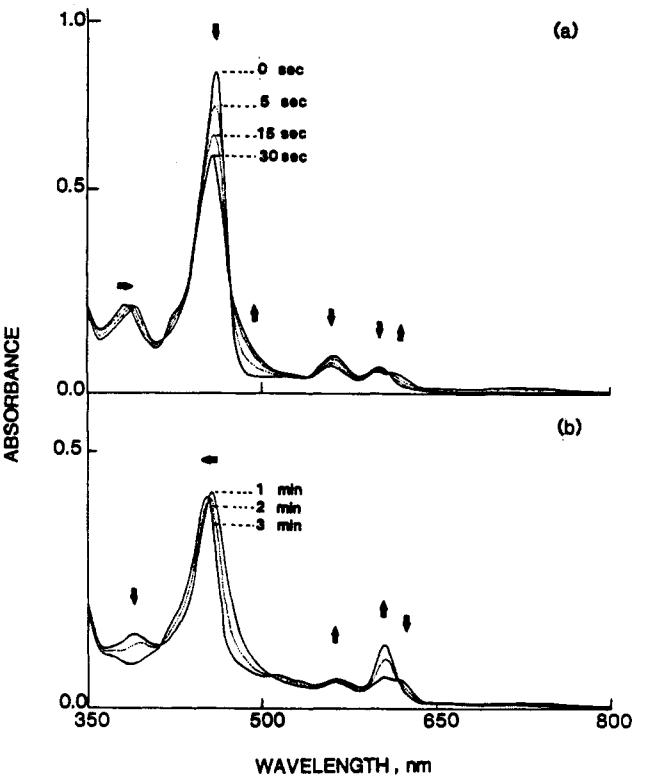

Figure 4. Thin-layer spectra obtained during controlled potential reduction of (TPP)Rh(CH_3)(PPh_3) at −1.65 V in CH_2Cl_2, containing 0.2 M TBAP and 1000 equiv of triphenylphosphine (a) between 0 and 30 s and (b) between 30 s and 3 min.

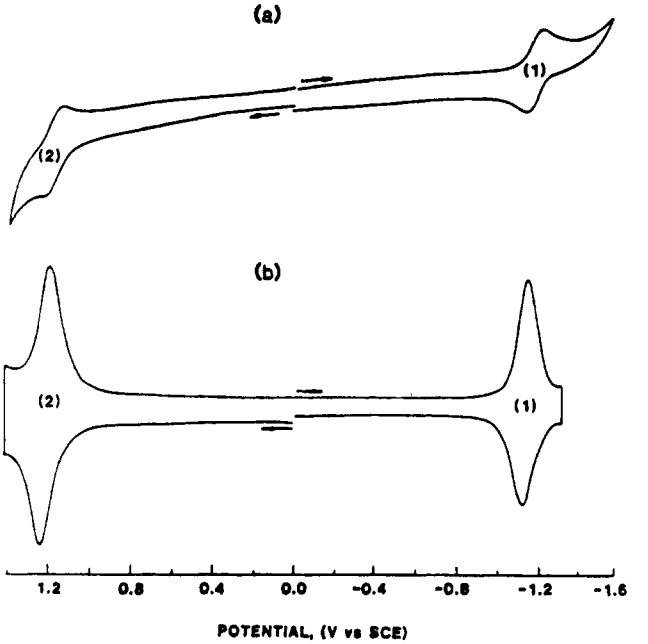

Figure 5. (a) Cyclic voltammogram of [(TPP)Rh($PPhMe_2$)$_2$]$^+$ in CH_2Cl_2, 0.1 M TBAP, at scan rate of 100 mV/s. (b) Differential pulse voltammetry of the same solution at a scan rate of 5 mV/s.

(13) Laitenen, M. A.; Harris, W. E. *Chemical Analysis*; McGraw-Hill: New York, 1975; p 227.
(14) Anderson, J. E.; Yao, C.-L.; Kadish, K. M. *Inorg. Chem.* **1986**, *25*, 718.

Table IV. UV-Visible Spectra of Transient [(P)Rh(R)(PPh$_3$)]$^-$ in CH_2Cl_2 Containing 0.2 M TBAP and 1000 Equiv of Uncomplexed PPh_3

compound[a]	λ_{max}, nm ($10^{-3}\epsilon$)				
[(TPP)Rh(CH_3)(PPh_3)]$^-$	379 (24.1)	437 (61.3)	549 (8.2)	594 (8.9)	608 (8.1)
[(TPP)Rh(C_2H_5)(PPh_3)]$^-$	379 (24.2)	437 (64.3)	549 (8.9)	594 (7.8)	608 (6.5)
[(TPP)Rh(C_4H_9)(PPh_3)]$^-$	379 (17.5)	437 (64.9)	549 (9.6)	594 (7.8)	608 (7.4)
[(OEP)Rh(CH_3)(PPh_3)]$^-$	367	427	531	561	

[a] Obtained after controlled potential reduction of (P)Rh(R)(PPh_3) at −1.65 V.

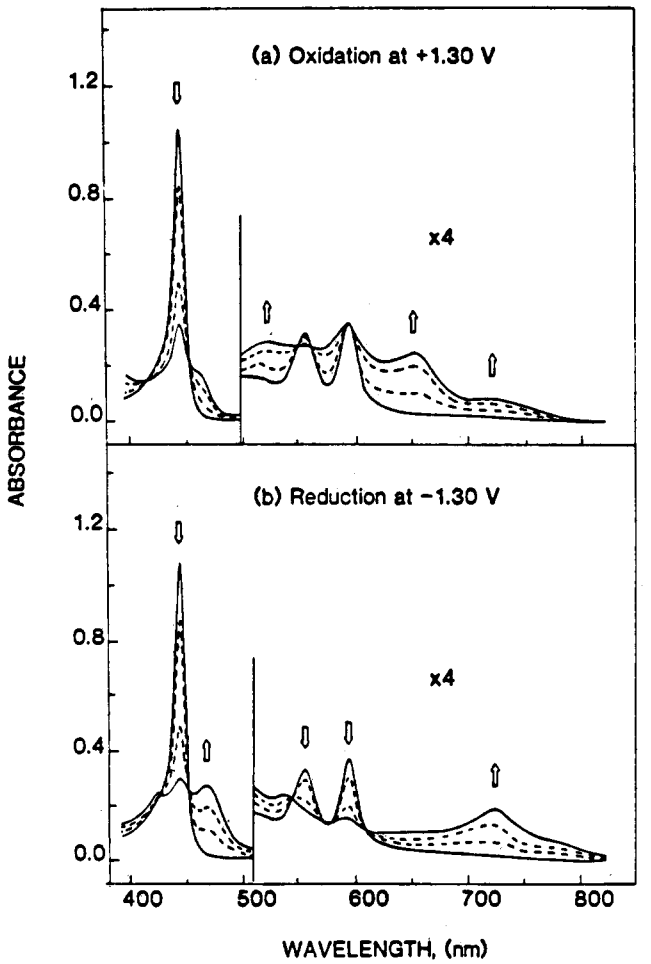

Figure 6. Time-resolved electronic absorption spectral changes of [(TPP)Rh(PPhMe$_2$)$_2$]$^+$ upon (a) controlled potential oxidation at +1.30 V and (b) controlled potential reduction at −1.30 V in CH_2Cl_2.

These data are shown in Table IV.

The spectrum of [(TPP)Rh(CH_3)(PPh_3)]$^-$ is only observed at experimental times between 0 and 30 s of electrolysis. This is shown in Figure 4a. At longer times, a new species is generated, and after 3 min the spectrum in CH_2Cl_2 is characterized by bands at 433, 549, and 594 nm. This is shown in Figure 4b. Reduction of the other (P)Rh(R)(PPh_3) species leads to an initial spectrum of [(P)Rh(R)(PPh_3)]$^-$, but the final reduced species all have the same UV-visible spectra. The final reduction product has not been assigned but may be associated with the generation of σ-bonded (TPP)Rh(CH_2Cl)(PPh_3) in CH_2Cl_2 (see ref 14). The reductions of (P)Rh(R)(PPh_3) were also spectrally monitored in PhCN and invariably led to spectra associated with dimeric [(P)Rh]$_2$. This also occurred after approximately 3 min of electrolysis.

Electrochemistry of [(TPP)Rh(PPhMe$_2$)$_2$]$^+$ in CH_2Cl_2. Figure 5a shows a cyclic voltammogram of [(TPP)Rh(PPhMe$_2$)$_2$]$^+$ in CH_2Cl_2, 0.1 M TBAP. There is a single reversible reduction at $E_{1/2}$ = −1.14 V and a single reversible oxidation at $E_{1/2}$ = +1.20 V. A reversible oxidation and reduction are also observed by differential pulse voltammetry as shown in Figure 5b.

The time-resolved spectral changes of [(TPP)Rh(PPhMe$_2$)$_2$]$^+$ at an applied potential +1.30 V are shown in Figure 6a while Figure 6b shows the changes that occur in the UV-visible spectra during controlled potential reduction at −1.30 V. These spectral data clearly indicate that a cation radical is formed upon oxidation. Unexpectedly, a radical is also formed upon reduction of [(TPP)Rh(PPhMe$_2$)$_2$]$^+$. This is evidenced by the decrease of the three absorption bands at 444, 555, and 594 nm and the appearance of a characteristic anion radical peak at 730 nm.

In summary, the data in this paper clearly demonstrate that the site of electroreduction in Rh porphyrins critically depends upon the nature of the fifth and sixth axial ligands. All complexes with a σ-bonded alkyl ligand are reduced at the porphyrin π-ring system while complexes of the type [(TPP)Rh(L)$_2$]$^+$ may undergo metal- or ring-centered reductions depending upon the specific properties of L. A metal-centered reduction and dimerization of the electrogenerated Rh(II) complex occurs when L is triphenylphosphine,[4] dimethylamine,[5] or pyridine.[5] On the other hand, when L is dimethylphenylphosphine, the formation of a π radical is clearly demonstrated. This suggests that the properties of dimethylphenylphosphine closely approximate those of the σ-bonded alkyl ligand when complexed to (TPP)Rh(R) or (TPP)Rh(R)(L). It is possible that similar electrochemical properties will be observed for other metalloporphyrins complexed by dimethylphenylphosphine. This is presently under investigation.

Acknowledgment. The support of the National Science Foundation (Grant No. CHE-8515411) is gratefully acknowledged.